6 Modal Analysis of Civil Engineering Structures

In general system identification of civil engineering structures serves as a tool for modal analysis as explained in the introduction. In modal analysis, it is the modal parameters of the dynamic modes of the structure that are sought. In chapter 3, it was shown how these parameters could be determined from the combined continuous-time system by means of a modal decomposition.

In section 6.1, it is shown how to obtain the modal parameters on the basis of an estimated discrete-time model. Further, by using the prediction error estimation approach, it is possible to estimate the uncertainties of the modal parameters associated with the identification of these. In some applications this additional information is very important. This will be the subject of section 6.2. In section 3.1.4, it was described how the dynamic properties of a continuous-time system can be illustrated by plotting the spectral densities of the system. In a similar manner, it is possible to visualize the spectral densities of the system by means of the estimated discrete-time model. The spectral density estimation using discrete-time stochastic models is the subject of section 6.3. One of the difficulties of modal analysis of ambient excited structures is that an identified model of such a system will contain physical as well as nonphysical modes. It is therefore necessary to assess whether an identified mode has physical origin or not. In section 6.4, it is shown how various approaches can be applied as an aid for this assessment.

Assume that the modal parameters of interest are the modal frequencies and the modal damping. Further, assume that all modes of interest of a structural system can be observed using only one sensor and that the system is subjected to an unknown ambient excitation. In such a case the system identification should be performed using an ARMA model according to the parsimony principle. The question is whether the information already obtained from such a system identification can be used if the mode shapes at a later state are desired. In most cases, it is in fact possible to use this information instead of performing a completely new system identification with an ARMAV model. In section 6.5, it is described how estimated ARMA models combined with FFT estimation of the covariance function of the measured system response can be used to obtain estimates of the mode shapes.

6.1 Modal Analysis of Civil Engineering Structures

This section will focus on obtaining estimates of the modal parameters of ambient excited civil engineering structures using ARMAV models or equivalent stochastic state space realizations. It is assumed, that the discrete-time model has been estimated using e.g. the PEM approach presented in chapter 5. The problem is how the modal parameters are related to the discrete-time models.

6.1.1 Modal Decomposition of Discrete-Time Systems

This section shows how to modally decompose a p-variate linear and time-invariant discrete-time system, represented by an arbitrary parametrized m-dimensional state space realization. Since this analysis only concerns the free vibrations of the system, it is unimportant whether the realization is of the innovation form or not. In any case the free vibrations are described by

$$\begin{aligned} \boldsymbol{x}(t_{k+1}) &= \boldsymbol{A}\boldsymbol{x}(t_k) \\ \boldsymbol{y}(t_k) &= \boldsymbol{C}\boldsymbol{x}(t_k) \end{aligned} \tag{6.1}$$

where the dimensions of the state vector $\boldsymbol{x}(t_k)$ and the output vector $\boldsymbol{y}(t_k)$ are $m \times 1$ and $p \times 1$, respectively. The solution of this system is assumed to be of the form

$$\boldsymbol{x}(t_k) = \boldsymbol{\psi}\mu^k \tag{6.2}$$

where $\boldsymbol{\psi}$ is an $m \times 1$ complex vector and μ is a complex constant. Insertion of (6.2) into (6.1) yields

$$\begin{aligned} \boldsymbol{\psi}\mu^{k+1} &= \boldsymbol{A}\boldsymbol{\psi}\mu^k \\ \boldsymbol{y}(t_k) &= \boldsymbol{C}\boldsymbol{\psi}\mu^k \end{aligned} \tag{6.3}$$

showing that (6.2) only is a solution if and only if $\boldsymbol{\psi}$ is a solution to the first-order eigenvalue problem

$$(\boldsymbol{I}\mu - \boldsymbol{A})\boldsymbol{\psi} = \boldsymbol{0} \tag{6.4}$$

This eigenvalue problem only has non-trivial solutions if the characteristic polynomial

$$det(\boldsymbol{I}\mu - \boldsymbol{A}) = 0 \tag{6.5}$$

is satisfied. The order of this real-valued polynomial is m. Thus, there will be m roots μ_j that are the eigenvalues of $\boldsymbol{A}$. For each of these eigenvalues there is a non-trivial solution vector $\boldsymbol{\psi}_j$ which is the corresponding eigenvector. The mode shape $\boldsymbol{\Phi}_j$, which is the observable part of the eigenvector, is then trivially obtained from the observation equation of (6.3) as

$$\boldsymbol{\Phi}_j = \boldsymbol{C}\boldsymbol{\psi}_j \,, \quad j = 1,\ 2,\ \ldots\ ,\ m \tag{6.6}$$

The complex modal matrix $\boldsymbol{\Psi}$ is obtained by assembling all m eigenvectors to yield

$$\boldsymbol{\Psi} = \left[\boldsymbol{\psi}_1 \;\; \boldsymbol{\psi}_2 \;\; . \;\; . \;\; . \;\; \boldsymbol{\psi}_m\right] \tag{6.7}$$

This matrix diagonalizes $\boldsymbol{A}$ into a diagonal matrix $\boldsymbol{\mu}$ that contains the m eigenvalues. In other words

$$\boldsymbol{\Psi}^{-1}\boldsymbol{A}\boldsymbol{\Psi} = \boldsymbol{\mu} \;, \quad \boldsymbol{\mu} = diag\{\mu_j\} \;, \quad j = 1,\; 2,\; \ldots \;,\; m \tag{6.8}$$

which by rearrangement defines the modal decomposition of $\boldsymbol{A}$ as

$$\boldsymbol{A} = \boldsymbol{\Psi}\boldsymbol{\mu}\boldsymbol{\Psi}^{-1} \tag{6.9}$$

If the state dimension m divided by the number of outputs p equals an integral value n, and if the system is observable, then it is possible to represent the free vibrations of (6.1) by an nth order p-variate auto-regressive matrix polynomial. According to (2.40), the auto-regressive coefficient matrices satisfies the relation

$$\mathbf{0} = \boldsymbol{C}\boldsymbol{A}^n + \boldsymbol{A}_1\boldsymbol{C}\boldsymbol{A}^{n-1} + \ldots + \boldsymbol{A}_{n-1}\boldsymbol{C}\boldsymbol{A} + \boldsymbol{A}_n\boldsymbol{C} \tag{6.10}$$

Inserting (6.9) into (6.10) yields

$$\begin{aligned} \mathbf{0} &= \boldsymbol{C}\boldsymbol{\Psi}\boldsymbol{\mu}^n\boldsymbol{\Psi}^{-1} + \boldsymbol{A}_1\boldsymbol{C}\boldsymbol{\Psi}\boldsymbol{\mu}^{n-1}\boldsymbol{\Psi}^{-1} + \ldots + \boldsymbol{A}_{n-1}\boldsymbol{C}\boldsymbol{\Psi}\boldsymbol{\mu}\boldsymbol{\Psi}^{-1} + \boldsymbol{A}_n\boldsymbol{C} \\ &= \boldsymbol{C}\boldsymbol{\Psi}\boldsymbol{\mu}^n + \boldsymbol{A}_1\boldsymbol{C}\boldsymbol{\Psi}\boldsymbol{\mu}^{n-1} + \ldots + \boldsymbol{A}_{n-1}\boldsymbol{C}\boldsymbol{\Psi}\boldsymbol{\mu} + \boldsymbol{A}_n\boldsymbol{C}\boldsymbol{\Psi} \end{aligned} \tag{6.11}$$

The last equation can be decomposed into m separate relations. Each of these has the form

$$\begin{aligned} \mathbf{0} &= \boldsymbol{C}\boldsymbol{\psi}_j\mu_j^n + \boldsymbol{A}_1\boldsymbol{C}\boldsymbol{\psi}_j\mu_j^{n-1} + \ldots + \boldsymbol{A}_{n-1}\boldsymbol{C}\boldsymbol{\psi}_j\mu_j + \boldsymbol{A}_n\boldsymbol{C}\boldsymbol{\psi}_j \\ &= \left(\boldsymbol{I}\mu_j^n + \boldsymbol{A}_1\mu_j^{n-1} + \ldots + \boldsymbol{A}_{n-1}\mu_j + \boldsymbol{A}_n\right)\boldsymbol{C}\boldsymbol{\psi}_j \\ &= \left(\boldsymbol{I}\mu_j^n + \boldsymbol{A}_1\mu_j^{n-1} + \ldots + \boldsymbol{A}_{n-1}\mu_j + \boldsymbol{A}_n\right)\boldsymbol{\Phi}_j \;, \quad j = 1,\; 2,\; \ldots \;,\; m \end{aligned} \tag{6.12}$$

and is seen to be an nth order eigenvalue problem for the auto-regressive matrix polynomial with μ_j being the eigenvalue and the mode shape $\boldsymbol{\Phi}_j$ being the solution vector.

So in conclusion:

☞ *If the p-variate m-dimensional discrete-time system* (6.1) *is observable and fulfils the above-mentioned dimensional requirement, then the system can be represented by a p-variate auto-regressive matrix polynomial of the order n. In this case the modal decomposition of the discrete-time system* (6.9) *will also be the modal decomposition of the associated auto-regressive matrix polynomial.*

If the state space system (6.1) is an observability canonical realization, see section 2.5.2, then the transition matrix $\boldsymbol{A}$ will be in companion form, see Gohberg et al. [30]. By comparing the jth eigenvalue problem in (6.12) with the structure of the companion matrix, see e.g. theorem 2.4, it is the easy to verify that the associated eigenvector is given by

$$\boldsymbol{\psi}_j = \begin{bmatrix} \boldsymbol{\Phi}_j \\ \mu_j \boldsymbol{\Phi}_j \\ . \\ . \\ \mu_j^{n-2} \boldsymbol{\Phi}_j \\ \mu_j^{n-1} \boldsymbol{\Phi}_j \end{bmatrix} \tag{6.13}$$

and that the complex modal matrix $\boldsymbol{\Psi}$ will be a Vandermonde matrix, see Gohberg et al. [30]. As seen, the modal decomposition of this realization resembles the modal decomposition of the combined continuous-time system (3.46). This system is also realised in the observability canonical form.

As with the continuous-time modal decomposition, it has implicitly been assumed that all eigenvalues are distinct, since this is a necessary assumption for $\boldsymbol{A}$ to be diagonalizable. The question is now:

☞ *How do the discrete-time eigenvalues and mode shapes relate to the modal parameters that describe the continuous-time system?*

A question that must be answered before the modal decomposed discrete-time system can be interpreted in terms of the modal parameters.

6.1.2 Modal Parameters of Discrete-Time Systems

In chapter 3, it was shown how the modal decomposition of the combined continuous-time system provides the foundation for modal analysis. However, it is the modal decomposition of the identified discrete-time system that is available, so it is necessary to establish the link between the two decompositions. This link is established through the definition of the transition matrix $\boldsymbol{A} = e^{\boldsymbol{F}T}$, given in (4.4). To ease the notation, let the complex modal matrix associated with $\boldsymbol{A}$, be defined as $\boldsymbol{\Psi}_{\boldsymbol{A}}$. If both sides of (4.4) is modally decomposed, the following result is obtained

$$\begin{aligned} \boldsymbol{\Psi}_{\boldsymbol{A}}\,\boldsymbol{\mu}\,\boldsymbol{\Psi}_{\boldsymbol{A}}^{-1} &= e^{\boldsymbol{\Psi}\,\boldsymbol{\lambda}\,\boldsymbol{\Psi}^{-1}T} \\ &= \boldsymbol{\Psi}\,e^{\boldsymbol{\lambda}T}\boldsymbol{\Psi}^{-1} \end{aligned} \tag{6.14}$$

From this relation, it is seen that the complex modal matrices $\boldsymbol{\Psi}_{\boldsymbol{A}}$ and $\boldsymbol{\Psi}$ are equivalent, except for an arbitrary scaling. Since the observation matrix of the discrete-time system is equal to the observation matrix of the combined continuous-time system, and since the mode shapes can be obtained as

$$\left[\boldsymbol{\Phi}_1 \quad \boldsymbol{\Phi}_2 \quad . \quad . \quad . \quad \boldsymbol{\Phi}_m\right] = \boldsymbol{C}\boldsymbol{\Psi} \tag{6.15}$$

it also follows, that the mode shapes of the discrete-time system are equivalent to the mode shapes of the continuous-time system, except for an arbitrary scaling. Finally, from (6.14) it is seen that the m eigenvalues of the two systems are related as

$$\mu_j = e^{\lambda_j T}, \quad j = 1,\ 2,\ \ldots\ ,\ m \tag{6.16}$$

In chapter 3 underdamped physical modes were assumed. Further, it was assumed that a modal frequency was characterized by the angular eigenfrequency ω_j or the natural eigenfrequency f_j, whereas the modal damping was characterized by the damping ratio ζ_j. From (6.16) and (3.8), these parameters are determined as

$$\left.\begin{aligned} \lambda_j &= \frac{log\,(\mu_j)}{T} \\ \omega_j &= |\lambda_j| \\ f_j &= \frac{|\lambda_j|}{2\pi} \\ \zeta_j &= -\frac{Re\,(\lambda_j)}{|\lambda_j|} \end{aligned}\right\} \quad j = 1,\ 3,\ \ldots\ ,\ 2s-1 \tag{6.17}$$

where *log* is the natural logarithm. It has been assumed that *s* complex conjugated pairs of eigenvalues has been identified as the eigenvalues of *s* underdamped physical modes, among all *m* eigenvalues. How these 2*s* eigenvalues are determined in practice is the subject of section 6.3. The modal vectors that correspond to these underdamped modes are characterized by the complex conjugated pair of scaled mode shapes. These are obtained from the eigenvectors of the modal decomposition using (6.15).

6.2 Estimation of Standard Deviations of Modal Parameters

In chapter 5 the PEM estimator of a discrete-time model was investigated. It was shown that the estimator was consistent as the number of samples N tend to infinity, if the true system was contained in the model and if the prediction errors were Gaussian white noise. In this case the estimated parameter $\hat{\boldsymbol{\theta}}_N$ will converge to the true system parameters $\boldsymbol{\theta}_0$ with probability 1, see Ljung [71], and the estimator will be asymtotically unbiased. It was also established that the PEM estimator will be statistically efficient for a certain choice of criterion function, if the true system is contained in the model, and if the prediction errors constitute a Gaussian white noise. A standard for the estimation errors of a statistically efficient estimator was shown to be provided by the Cramer-Rao lower bound. This standard was utilized by the covariance matrix $\boldsymbol{P}_\theta(\hat{\boldsymbol{\theta}}_N) = E[(\boldsymbol{\theta}_0 - \hat{\boldsymbol{\theta}}_N)(\boldsymbol{\theta}_0 - \hat{\boldsymbol{\theta}}_N)^T]$ of the difference between $\boldsymbol{\theta}_0$ and $\hat{\boldsymbol{\theta}}_N$ as N tends to infinity. A reasonable estimate of $\boldsymbol{P}_\theta(\hat{\boldsymbol{\theta}}_N)$ that can be obtained directly from the PEM estimator was given by (5.50) as

$$\hat{\boldsymbol{P}}_\theta(\hat{\boldsymbol{\theta}}_N) = \boldsymbol{R}^{-1}(\hat{\boldsymbol{\theta}}_N) \tag{6.18}$$

where $\boldsymbol{R}_N(\hat{\boldsymbol{\theta}}_N)$ is obtained from the approximated Hessian, which is calculated of the basis of the measurements and the estimated parameters.

This section investigates how to transform the estimation errors represented by the covariance matrix $\hat{\boldsymbol{P}}_\theta(\hat{\boldsymbol{\theta}}_N)$ to estimate uncertainties of the modal parameters. This additional information can be important in different applications. In the next section, one of these applications will be illustrated. In any case, having a qualitative measure of the accuracy of the estimated modal parameters makes it possible to assess their quality. The modal decomposition of the homogeneous part of any discrete-time system is simply a convenient change of parameterization of the model since the modal parameters can be interpreted physically. This is impossible to do for the model parameters $\hat{\boldsymbol{\theta}}_N$. In general this change of parameterization from a set of model parameters given in an $m \times 1$ dimensional vector $\boldsymbol{\theta}$ to another set of physical parameters given in an $n \times 1$ dimensional vector $\boldsymbol{\kappa}$ can be performed by a known n-dimensional functional relation

$$\boldsymbol{\kappa} = \boldsymbol{f}(\boldsymbol{\theta}) \tag{6.19}$$

The dimensions of $\boldsymbol{\theta}$ and $\boldsymbol{\kappa}$ are in general different. There will typically be fewer physical parameters than model parameters, i.e. $m > n$, and obviously the accuracy and thus the sensitivity of $\boldsymbol{\kappa}$ is more significant than that of $\boldsymbol{\theta}$. In addition, the functional relation (6.19) will in general be nonlinear as in the case of the modal decomposition. Thus, to obtain a practically applicable approach, (6.19) is usually linearized using a first-order generalized Taylor expansion at the operating point $(\hat{\boldsymbol{\kappa}}_N, \hat{\boldsymbol{\theta}}_N)$, see Jensen et al. [45] and Knudsen [62]

$$\begin{aligned} \boldsymbol{\kappa} &= \hat{\boldsymbol{\kappa}}_N + \left(\frac{\partial \boldsymbol{f}(\boldsymbol{\theta})}{\partial \boldsymbol{\theta}} \right)_{|\boldsymbol{\theta} = \hat{\boldsymbol{\theta}}_N} \left(\boldsymbol{\theta} - \hat{\boldsymbol{\theta}}_N \right) \\ &= \hat{\boldsymbol{\kappa}}_N + \boldsymbol{J}(\hat{\boldsymbol{\theta}}_N)\left(\boldsymbol{\theta} - \hat{\boldsymbol{\theta}}_N \right) \end{aligned} \tag{6.20}$$

where $\boldsymbol{J}(\hat{\boldsymbol{\theta}}_N)$ is a Jacobian matrix of partial derivatives

$$\boldsymbol{J}(\boldsymbol{\theta}) = \begin{bmatrix} \frac{\partial f_1(\boldsymbol{\theta})}{\partial \theta_1} & \frac{\partial f_1(\boldsymbol{\theta})}{\partial \theta_2} & \cdot & \cdot & \frac{\partial f_1(\boldsymbol{\theta})}{\partial \theta_m} \\ \frac{\partial f_2(\boldsymbol{\theta})}{\partial \theta_1} & \frac{\partial f_2(\boldsymbol{\theta})}{\partial \theta_2} & \cdot & \cdot & \frac{\partial f_2(\boldsymbol{\theta})}{\partial \theta_m} \\ \cdot & \cdot & \cdot & \cdot & \cdot \\ \cdot & \cdot & \cdot & \cdot & \cdot \\ \frac{\partial f_n(\boldsymbol{\theta})}{\partial \theta_1} & \frac{\partial f_n(\boldsymbol{\theta})}{\partial \theta_2} & \cdot & \cdot & \frac{\partial f_n(\boldsymbol{\theta})}{\partial \theta_m} \end{bmatrix} \tag{6.21}$$

which should be evaluated at the operating point $\hat{\boldsymbol{\theta}}_N$. The deviation of the estimate $\hat{\boldsymbol{\kappa}}_N$ from the true parameters $\boldsymbol{\kappa}_0$ can as such be evaluated from (6.20) as

$$\boldsymbol{\kappa}_0 - \hat{\boldsymbol{\kappa}}_N = \boldsymbol{J}(\hat{\boldsymbol{\theta}}_N)\left(\boldsymbol{\theta}_0 - \hat{\boldsymbol{\theta}}_N \right) \tag{6.22}$$

implying that the covariance matrix $\boldsymbol{P}_{\boldsymbol{\kappa}}(\hat{\boldsymbol{\kappa}}_N)$ of the deviation of $\hat{\boldsymbol{\kappa}}_N$ from the true parameters can be estimated by

$$\begin{aligned} \hat{\boldsymbol{P}}_{\boldsymbol{\kappa}}(\hat{\boldsymbol{\kappa}}_N) &= E\left[\left(\boldsymbol{\kappa}_0 - \hat{\boldsymbol{\kappa}}_N \right)\left(\boldsymbol{\kappa}_0 - \hat{\boldsymbol{\kappa}}_N \right)^T \right] \\ &= \boldsymbol{J}(\hat{\boldsymbol{\theta}}_N) E\left[\left(\boldsymbol{\theta}_0 - \hat{\boldsymbol{\theta}}_N \right)\left(\boldsymbol{\theta}_0 - \hat{\boldsymbol{\theta}}_N \right)^T \right] \boldsymbol{J}^T(\hat{\boldsymbol{\theta}}_N) \\ &= \boldsymbol{J}(\hat{\boldsymbol{\theta}}_N) \boldsymbol{P}_{\boldsymbol{\theta}}(\hat{\boldsymbol{\theta}}_N)\, \boldsymbol{J}^T(\hat{\boldsymbol{\theta}}_N) \end{aligned} \tag{6.23}$$

The estimated covariance matrix $\hat{\boldsymbol{P}}_{\boldsymbol{\theta}}(\hat{\boldsymbol{\theta}}_N)$ obtained from (6.18) can then be inserted instead of $\boldsymbol{P}_{\boldsymbol{\theta}}(\hat{\boldsymbol{\theta}}_N)$. This expression will only be accurate if $\hat{\boldsymbol{P}}_{\boldsymbol{\theta}}(\hat{\boldsymbol{\theta}}_N)$ is a good estimate

of $\boldsymbol{P}_\theta(\hat{\theta}_N)$ and if the error due to the linear approximation is small. What remains is to calculate the Jacobian matrix $\boldsymbol{J}(\hat{\theta}_N)$. This is in general impossible to do analytically even for small model structures, when the physical parameters of interest are the modal parameters. It is therefore necessary to rely on numerical differentiation. It should be remembered, that the modal parameters are only sensitive to changes in the parameters that relate to the homogeneous part of the model structure. This subset of the estimated parameters will be denoted $\hat{\theta}_N^H$. This also imply that only a subset of the rows and columns of $\boldsymbol{P}_\theta(\hat{\theta}_N)$ should be used. In the case of an ARMAV model $\hat{\theta}_N^H$ will only include the auto-regressive parameters, and for a general stochastic state space realization it will include the non-trivial parameters of the matrix pair $\{\boldsymbol{A},\boldsymbol{C}\}$.

6.2.1 Natural Eigenfrequencies and Damping Ratios

It is usually only the estimated standard deviations of the modal parameters that are of interest. This simplifies the calculation of the Jacobian matrix, since the calculations of the standard deviations of the natural eigenfrequencies and damping ratios can be separated from the calculations of the standard deviations of the scaled mode shapes. Define the elements of $\hat{\kappa}_N$ as the estimated natural eigenfrequencies and associated damping ratios of the model. These parameters were obtained in (6.17) in section 6.1.2, under the assumption that s complex conjugated pairs of eigenvalues describe the s structural modes of the model. In other words

$$\hat{\kappa}_N = \begin{bmatrix} f_1 & \zeta_1 & f_2 & \zeta_2 & . & . & . & f_s & \zeta_s \end{bmatrix}^T \tag{6.24}$$

The functional relationship between these parameters and the model parameters is given by the eigenvalue problem (6.4) in section 6.1.1, followed by the calculation of the modal parameters given in (6.17). This means that the resulting functional relation between the model and modal parameters is highly nonlinear. A reasonable way to calculate the Jacobian is by use of numerical differentiation using the central difference theorem. The ith column of the $2s \times m$ matrix $\boldsymbol{J}(\hat{\theta}_N^H)$ can then be calculated by

$$\boldsymbol{J}_i(\hat{\theta}_N^H) = \frac{\boldsymbol{f}(\hat{\theta}_N^H + \boldsymbol{P}) - \boldsymbol{f}(\hat{\theta}_N^H - \boldsymbol{P})}{2\boldsymbol{P}_i} \tag{6.25}$$

where $\boldsymbol{P}$ is an $m \times 1$ vector whose elements all are zero except the ith element $\boldsymbol{P}_i$ that contains a small number. This number results in a small perturbation of the ith element of $\hat{\theta}_N^H$. The modal decomposition and the calculation of the modal parameters must therefore be repeated $2m$ times. The estimated covariance matrix of the modal parameters $\hat{\boldsymbol{P}}_\kappa(\hat{\kappa}_N)$ is the obtained from (6.23), and the standard deviations can be extracted from the diagonal elements.

6.2.2 Scaled Mode Shapes

As with the natural eigenfrequencies and the associated damping ratios, it is also possible to estimate the standard deviations of scaled mode shapes. The additional computational effort in doing this is insignificant since the repeated number of modal decompositions are performed anyway in the estimation of the standard deviations of the natural eigenfrequencies and damping ratios. The vector $\hat{\boldsymbol{\kappa}}_N$ is now defined in terms of the normalized mode shapes $\boldsymbol{\phi}_j$ as

$$\hat{\boldsymbol{\kappa}}_N = \left[\boldsymbol{\phi}_1^T \;\; \boldsymbol{\phi}_2^T \;\; . \;\; . \;\; . \;\; \boldsymbol{\phi}_s^T\right]^T \tag{6.26}$$

These mode shapes are obtained from the $p \times 1$ scaled mode shapes $\boldsymbol{\Phi}_j$ by normalization of $\boldsymbol{\Phi}_j$ with respect to one of its p coordinates, i.e.

$$\boldsymbol{\phi}_j = \frac{1}{\Phi_{j,i}}\boldsymbol{\Phi}_j \;, \quad i \in [1,\, p] \tag{6.27}$$

In this way the uncertainty of the coordinates of the mode shapes is relative to the fixed deterministic ith coordinate. Due to the otherwise arbitrary scaling of the mode shapes, this is a necessary step before the Jacobian matrix can be calculated using the numerical differentiation approach. There will as such be s elements of $\hat{\boldsymbol{\kappa}}_N$ that are deterministic. This means that s rows and columns of the estimated covariance matrix $\hat{\boldsymbol{P}}_{\boldsymbol{\kappa}}(\hat{\boldsymbol{\kappa}}_N)$ will be zero because s rows of the $sp \times m$ matrix $\boldsymbol{J}(\hat{\boldsymbol{\theta}}_N^H)$ will be zero. The square roots of the diagonal elements of $\hat{\boldsymbol{P}}_{\boldsymbol{\kappa}}(\hat{\boldsymbol{\kappa}}_N)$ will then be the standard deviations of the mode shape coordinates relative to the fixed coordinate. In the first experimental case in chapter 8, which is a simulation study, the performance of the above techniques for estimation of the uncertainties of the estimated modal parameters will be analysed for a multivariate case.

6.3 Spectrum Analysis of Civil Engineering Structures

In section 3.1.4, it was shown how the spectral densities of a continuous-time stochastic system could be calculated and applied as an efficient tool for visualization of the dynamic properties of the system and its excitation. In a similar manner, it is possible to estimate the spectral densities of a sampled system. This spectral density estimation is usually performed by FFT, which is a fast way to obtain a sensible estimate of the spectral densities. However, as pointed out in section 1.1.1 the FFT has some drawbacks. These are limited frequency resolution and leakage in case of non-periodic data. In order to reduce the leakage problem in case of non-periodic data, the data were windowed prior to the FFT. If a modal analysis is based on FFT-based spectral densities, the results will according to section 1.1.1 be modal frequency estimates with limited accuracy and overestimated modal damping estimates due to the leakage and the windowing. In general, if the FFT spectral density estimates are only used for visualization purposes these drawbacks will not

be severe. However, closely spaced modes might be very difficult to detect due the limited frequency resolution and the possible leakage.

For ambient excited structures it is usually only possible to estimate the spectral densities of the system response, since the actual excitation is unknown. In this case the spectral densities of an estimated parametric model provides a good alternative to any FFT-based approach. Since the parametric models are estimated directly in time domain, and since they do not assume periodic data, no leakage will occur and windowing will as such be unnecessary. This results in more accurate modal frequencies and better estimates of the modal damping, see e.g. Pandit [84] and Pandit et al. [89]. Further, due to the parametric nature of the discrete-time models, and the fact that they also account for the presence of noise, there will not be the same limitations of the frequency resolution as experienced with the FFT. If the identified parametric model is covariance equivalent with the true system, the spectral densities will also be correct compared to those of the true system due to the Wiener-Khinchin relation, see e.g. Bendat et al. [14]. Further, since the system is described by parameters the spectral densities will be described by polynomials, and will as such have a smooth appearance.

The improved estimates of modal parameters and spectral densities do not come for free. The computational effort in obtaining these estimates is significantly larger, both in computational time and memory requirements. Further, the use of FFT is simple compared to discrete-time modelling. This is due to the somewhat iterative process needed to determine the optimal model. Therefore, it must be emphasized, that the use of e.g. ARMAV models in modal and spectrum analysis, should not regarded as a replacement of the traditional FFT-based techniques. It should merely be taken as an additional tool that in some cases can provide a more accurate description of the dynamics of a system. For this reason, modal and spectrum analysis of sampled data should always start by an examination of results obtained using the FFT. Plotting the FFT-based spectral densities together with the spectral densities obtained from the parametric model provides an efficient validation tool for the adequacy of the identified model. Therefore, it is in this section shown how to obtain the spectral densities of an identified discrete-time parametric model.

6.3.1 Spectrum Analysis using Discrete-Time Systems

In this section the spectrum analysis of ambient excited structures is considered. Since the actual excitation is unknown, spectrum analysis of ambient excited structures is concentrated on the estimation of the spectral densities of the output. Assume that an adequate discrete-time model has been estimated. Let this model be represented by a stochastic innovation state space realization as

$$\begin{aligned} \hat{\boldsymbol{x}}(t_{k+1}|t_k) &= \boldsymbol{A}\hat{\boldsymbol{x}}(t_k|t_{k-1}) + \boldsymbol{K}\boldsymbol{e}(t_k)\ , \quad \boldsymbol{e}(t_k) \in NID(\boldsymbol{0},\boldsymbol{\Lambda}) \\ \boldsymbol{y}(t_k) &= \boldsymbol{C}\hat{\boldsymbol{x}}(t_k|t_{k-1}) + \boldsymbol{e}(t_k) \end{aligned} \tag{6.28}$$

As shown in chapter 4, the true innovation process $\boldsymbol{e}(t_k)$ is only defined in terms of its statistical properties. Since $\boldsymbol{e}(t_k)$ is assumed to be a zero-mean Gaussian distributed process, both $\boldsymbol{y}(t_k)$ and $\boldsymbol{e}(t_k)$ are fully described by their covariance functions. In other words, the covariance function $\boldsymbol{\Sigma}(s)$ gives a complete statistical description of the system output $\boldsymbol{y}(t_k)$. By using the results of theorem A.2 in appendix A.3, the covariance function $\boldsymbol{\Sigma}(s)$ is described as

$$\boldsymbol{\Sigma}(s) = \begin{cases} \boldsymbol{C}\boldsymbol{\Pi}(0)\boldsymbol{C}^T + \boldsymbol{\Lambda} & , \quad s = 0 \\ \boldsymbol{C}\boldsymbol{A}^{s-1}\boldsymbol{M} & , \quad s > 0 \end{cases} \tag{6.29}$$

where $\boldsymbol{M}$ is defined by

$$\boldsymbol{M} = \boldsymbol{A}\boldsymbol{\Pi}(0)\boldsymbol{C}^T + \boldsymbol{K}\boldsymbol{\Lambda} \tag{6.30}$$

and the covariance matrix $\boldsymbol{\Pi}(0)$ being a positive definite solution of the Lyapunov equation

$$\boldsymbol{\Pi}(0) = \boldsymbol{A}\boldsymbol{\Pi}(0)\boldsymbol{A}^T + \boldsymbol{K}\boldsymbol{\Lambda}\boldsymbol{K}^T \tag{6.31}$$

For a p-variate system, the spectral densities of the output $\boldsymbol{y}(t_k)$ will be described by $p \times p$ spectral matrices $\boldsymbol{S}_{yy}(\omega)$, where ω is an arbitrary, angular frequency. As a consequence of the Wiener-Khinchin relation, the spectral densities can be obtained from the covariance function by a Fourier transformation of (6.29) to yield

$$\boldsymbol{S}_{yy}(\omega) = \left(\boldsymbol{C}\left(\boldsymbol{I}e^{i\omega} - \boldsymbol{A}\right)^{-1}\boldsymbol{K} + \boldsymbol{I}\right)\boldsymbol{\Lambda}\left(\boldsymbol{C}\left(\boldsymbol{I}e^{i\omega} - \boldsymbol{A}\right)^{-1}\boldsymbol{K} + \boldsymbol{I}\right)^H \tag{6.32}$$

The diagonal elements of $\boldsymbol{S}_{yy}(\omega)$ are the auto-spectral densities, whereas the off-diagonal elements are the cross-spectral densities which are complex in general. As it is the case of the covariance function, the following relation holds for the spectral densities $s_{yy}(\omega) = \boldsymbol{S}_{yy}^{\boldsymbol{H}}(-\omega)$. The superscript ^{H} signifies Hermitan transpose, i.e. transposition and complex conjugation. Since the eigenvalues of $\boldsymbol{A}$ are assumed to be inside the complex unit circle the spectral densities of all frequencies ω can be calculated. This is because the Fourier transform is evaluated on the complex unit circle. However, if the absolute value of ω exceeds the Nyquist frequency, aliasing will occur. The second-order properties given in frequency domain will also provide a full description of the system response. Plotting the spectral densities of the response is therefore a strong graphical tool for investigation of the dynamics of the combined system. This is especially true when lightly damped systems are represented by parametric models. In these cases the modes of the system will be sharp peaks and even closely spaced modes will have distinct peaks.

6.4 Identifying Structural Modes

This section concerns how to separate the structural part from the rest of an identified model, i.e. how to distinguish between physical and nonphysical modes. As will be shown there is no unique way of doing this. Several criteria exist, see e.g. Lembregts et al. [69] and Pandit [84], and this section will only introduce a subset of these.

6.4.1 Mode Identification using Eigenvalues

Common to most civil engineering structures experienced in real life applications is that they are underdamped. The damping ratios are typically not more than a few per cent. At the same time ambient excitation is typically of a broad-banded nature, which is modelled by a few critical or overdamped excitation "modes". This creates two natural selection criteria for a mode, which are:

☞ *Is the estimated damping of the mode not more than a few per cent?*
☞ *Is the mode described by a complex conjugated pair of eigenvalues?*

If the answers are affirmative there is a strong indication that the mode is of physical origin, since it is underdamped. These physical modes may be considered as the fundamental dynamic properties of the system, since most of the energy of the system is concentrated around these modes.

Consider an identified model having a number of such fundamental modes and assume that its state space dimension is larger than the dimension of the true system. If a new model with an increased state space dimension is identified, these modes will not be significantly improved. A larger model will instead add new information to the model about the minor dynamic components contained in the data, i.e. the disturbance. As the state space dimension increases, it offers more flexibility to the model for description of the dynamic properties of the system as given by the measured data. System properties properly described by a lower order model should be retained in the higher order models. This fact provides a third selection criterion if several identified models are available.

Assume that the identified models are sorted with respect to increasing state space dimension or AR order. It is then easy to identify the fundamental modes by plotting the increasing model orders versus the estimated eigenfrequencies. Such a plot is called a stability diagram, since it is easy to identify the stabilized, i.e. fundamental, modes contained in the models. Identified models that have been rejected by e.g. the Akaike's FPE test, see chapter 5, can as such provide valuable information in the selection of the structural modes of the optimal model.

In figure 6.1 a stability diagram with eight different ARMAV models is shown. All modes are marked with a dot and all modes having damping ratios less than 10% are marked with circles.

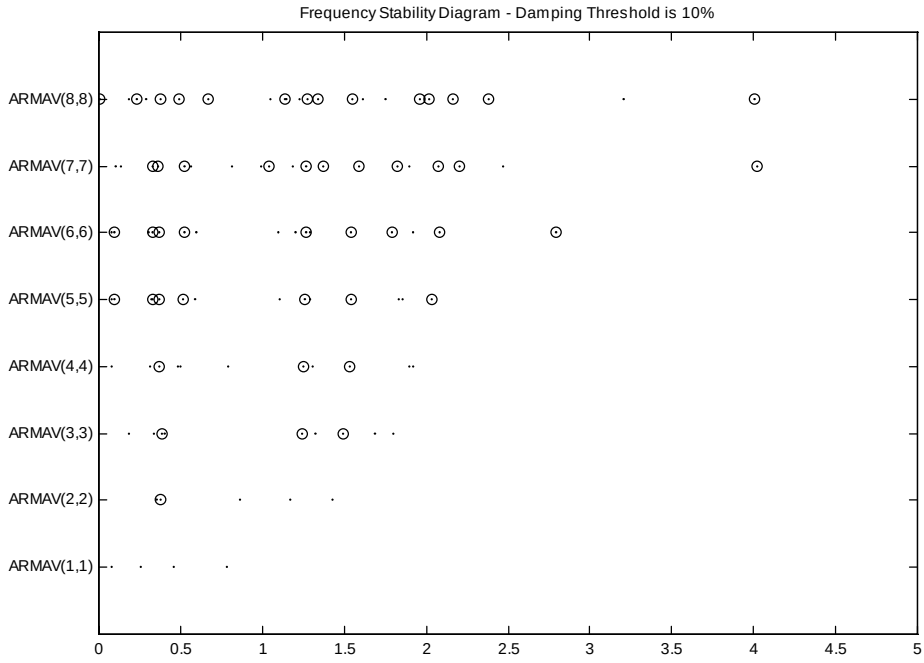

Figure 6.1: Frequency stability diagram using eight different ARMAV models. [o] - A mode having a damping ratios less than 10%. [•] - All identified modes of the models.

6.4.2 Mode Identification using Mode Shapes

The stability diagram can be refined by incorporating a priori knowledge into it. This a priori knowledge could e.g. be the amount of damping. If the damping ratio is less than a few per cent the mode could e.g. be plotted with another symbol. In this way the stability diagram will reveal all fundamental underdamped modes. The stability diagram is therefore a powerful visual tool for identification of the structural modes. So far all selection criteria have been based on the estimated eigenvalues. If multivariate models are estimated, the mode shapes will also provide some important geometrical knowledge about the modes. If a spatial model of the system is constructed and if it is animated by the complex mode shapes then it is possible to find at least the lower structural modes among the nonphysical modes. As the eigenfrequencies of the fundamental modes will repeat themselves when estimating several models with increasing state space dimension so will their scaled mode shapes. This means that the fundamental modes can be identified additionally by the agreement of the mode shapes of the different models. By introducing a measure of agreement between two vectors, it is possible to visualize using a stability diagram. The measure of agreement can e.g. be the Modal Assurance Criterion (MAC), see Allemang et al. [3]. Consider two p-variate models having the state space dimensions n and m, respectively. Denote the complex modal matrices, obtained by modal decomposition of the models, by $\mathbf{\Psi}_1$ and $\mathbf{\Psi}_2$. $\mathbf{\Psi}_1$ will as such have the dimension $p \times n$ and include the n scaled mode shapes $\mathbf{\Phi}_{j,1}$ of the first model. $\mathbf{\Psi}_2$ will in a similar

manner include the m scaled mode shapes $\mathbf{\Phi}_{j,2}$ of the second model, and its dimension will be $p \times m$. The MAC between these two models will then be a matrix having the dimensions $n \times m$. The (i,j)th element of it is defined in terms of the mode shapes $\mathbf{\Phi}_{j,1}$ and $\mathbf{\Phi}_{j,2}$ as

$$\boldsymbol{MAC}(i,j) = \frac{|\mathbf{\Phi}_{i,1}^H \mathbf{\Phi}_{j,2}|}{\sqrt{|\mathbf{\Phi}_{i,1}^H \mathbf{\Phi}_{i,1}|}\sqrt{|\mathbf{\Phi}_{j,1}^H \mathbf{\Phi}_{j,1}|}} \tag{6.33}$$

which is a real number between 0 and 1, see Allemang et al. [3]. If the $\boldsymbol{MAC}(i,j)$ is close to 1 there is a strong correlation between the two mode shapes, i.e. there is a strong possibility that they represent the same mode. If $m > n$ the maximum MAC number of each of the m columns of the MAC matrix then shows how well the mode shapes of the second model correlate with some of the mode shapes of the first model. The procedure can then be repeated for a third model, where the is calculated between the second and the third model. The result is a vector of maximum MAC numbers between the mode shapes of the current and the previous model. These MAC numbers can then be used to construct a stability diagram. All that is needed are at least two identified models. If the MAC value of a mode exceeds a threshold of e.g. 0.9 the value can be plotted by a symbol that is different from the symbol that would be used if the value was below the threshold. In this way it is easy to identify the fundamental modes on the basis of the mode shapes. Figure 6.6 shows how the MAC can be used to form a stability diagram.

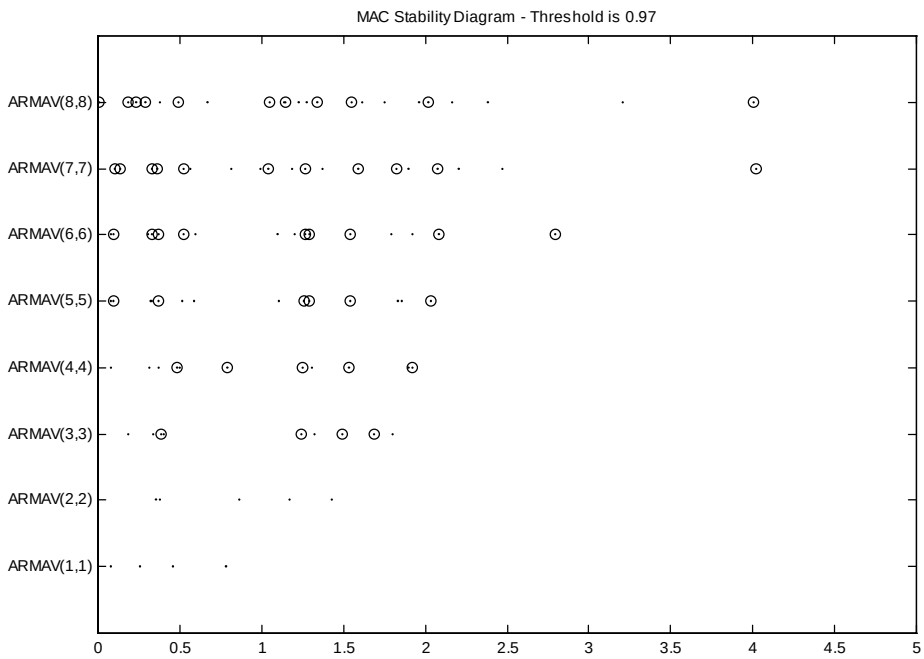

Figure 6.2: MAC stability diagram using eight different ARMAV models. [o] - A mode shape having a MAC value higher than 0.95 with a mode shape of the previously identified model. [•] - All identified modes of the models.

6.4.3 Other Methods for Mode Identification

Many other mode indicator functions exist. If the structural system e.g. is lightly damped, the corresponding mode shapes should be almost normal, i.e. the phase angles should be either $0°$ or $\pm 180°$. This can e.g. be checked by the Modal Phase Colinearity index (MPC), see Juang et al. [47]. Another type of indicator function is the so-called Modal Confidence Factor (MCF), see Ibrahim [40] and Vold et al. [110]. This indicator will be close to unity for structural mode shapes, whereas nonphysical modes will have an MCF of arbitrary phase and amplitude.

Assume that a multivariate parametric model has been applied to the identification of a structural system having closely spaced modes. Such a structural system could e.g. be an axisymmetric building. Closely spaced modes are used here as synonyms for the more mathematically correct term, which is repeated or pseudo-repeated eigenvalues. The Singular Value Decomposition (SVD) provides an efficient tool for the identification of closely spaced modes.

Any matrix $\boldsymbol{A}$ can be decomposed into a product of three matrices $\boldsymbol{U}$, $\boldsymbol{W}$ and $\boldsymbol{V}$ as $\boldsymbol{A} = \boldsymbol{U}\boldsymbol{W}\boldsymbol{V}^T$. These matrices have important characteristics that are useful in describing the system that is characterized by $\boldsymbol{A}$. The three matrices of the SVD have special characteristics. Both $\boldsymbol{U}$ and $\boldsymbol{V}$ are unitary, i.e. $\boldsymbol{U}^T\boldsymbol{U} = \boldsymbol{V}^T\boldsymbol{V} = \boldsymbol{I}$ and $\boldsymbol{V}\boldsymbol{V}^T = \boldsymbol{I}$. $\boldsymbol{W}$ is a diagonal matrix where a value on the diagonal corresponds to the magnitude of the dot product of the corresponding columns of the $\boldsymbol{U}$ and $\boldsymbol{V}$ matrices. These diagonal elements are called the singular values, and the magnitude of these decreases as the column number increases. This means that the first column in the $\boldsymbol{U}$ and $\boldsymbol{V}$ matrix is the major contributor of the $\boldsymbol{A}$ matrix. In many applications the column and/or rows of the $\boldsymbol{A}$ matrix is the superposition of a number of underlying vectors. Therefore, the singular values can be used to determine the number of significant underlying vectors which describe a system. The SVD can therefore be used as a mode indicator function.

By taking the SVD of the spectral density matrix $\boldsymbol{S}_{yy}(\omega)$ in (6.32), which was given section 6.3.1, the number of significant modes at the frequency ω can be detected. In the valleys of the spectral density plots there will be many significant singular values, since a lot of different modes play a role. However, around the peaks there will only be as many significant singular values as there are modes having resonance at that particular peak frequency. This provides a way of determining how many modes a certain peak is based on, i.e. a simple way of visual detection of closely spaced modes. In figure 6.3 the singular values of the spectral densities of a 2-channel ARMAV(5,5) model are plotted. The plot reveals a total of five significant modes. As seen there are two sets of closely spaced modes.

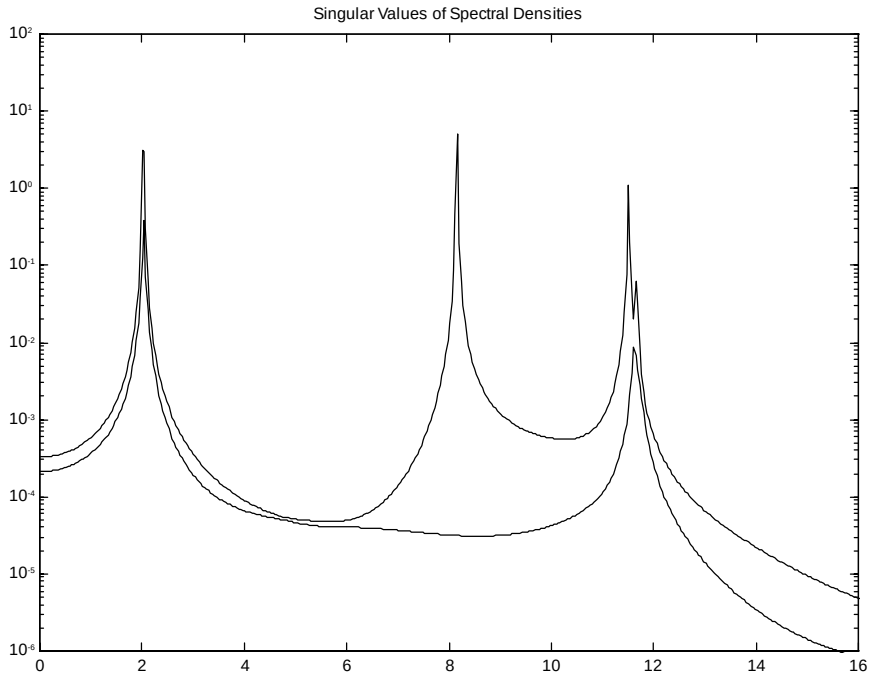

Figure 6.3: Singular values plot of the spectral densities of a 2-channel ARMAV(5,5) model.

Plotting of the spectral densities of the multivariate models with a high frequency resolution will usually reveal any closely spaced modes. Especially, amplitude plots of cross-spectral densities. However, the SVD approach provides an efficient way of counting the actual number of closely spaced modes. It is also possible to combine e.g. the MAC and the SVD in the search for closely spaced modes, see Philips et al. [90].

6.5 A Hybrid Modal Analysis Approach

In several cases a dynamic analysis of a structure restricts to the analysis of the modal frequencies and the corresponding damping. In other words, the determination of the scaled mode shapes is not of primary interest. In principle, it is possible to estimate all modal frequencies and corresponding modal damping from one measured data record, i.e. one measurement channel. This raises the question:

☞ *Is it ever necessary to apply a multivariate discrete-time model if only the modal frequencies and the modal damping are of interest?*

In modal analysis of ambient excited structures this question can be reformulated as to whether or not it is ever necessary to apply an ARMAV model instead of an ARMA model. From the system identification point of view this is an important question, since the number of parameters describing the univariate models is

significantly lower than the number of parameters of an equivalent multivariate model. An n-DOF univariate noise-free system is e.g. described by a univariate ARMA($2n$,$2n$-1) having $4n$-1 free parameters. This system can equivalently be described by an n-variate ARMAV(2,1) model having $3n^2$ free parameters. If the ARMA model is used, the bias can be reduced according to the parsimony principle, as explained in chapter 5. The answer to the question certainly depends on the structure as well as the measurements. If the structure is axisymmetric, which is the case for e.g. chimneys and masts, there might be several closely spaced modes. Such modes will be very difficult to detect if measurements from several locations and directions are unavailable. Thus, if the structure has closely spaced modes it is in general necessary to use a multivariate model. In these situations the different modes are most easily determined by an investigation of the associated mode shapes, which is the extra geometrical information provided by the multivariate model.

If the structure has well-separated modes, it is not necessary to use the multivariate models. However, caution must be taken to place the sensor at a location where all the modes of interest are observable. In other words, the sensor must not be located at the node points of any of these modes. Now assume that an ARMA model has been applied to determine the eigenfrequencies and damping ratios of a structure as a consequence of e.g. a satisfaction of the parsimony principle. The question is then whether this result can be used later on to determine the mode shapes of the structure in a simple way, if e.g. more measurement records at other locations become available, or whether it is necessary to identify an ARMAV model in order to obtain this extra information.

This section will show how the information already obtained using the ARMA model can be used as part of an estimation of the mode shapes by use of the new information obtained at other sensor locations. In the following it is assumed that p measurement records are available, and that an adequate ARMA model has been identified. From this model, it is then assumed that n complex conjugated pairs of eigenvalues $\{\mu_j,\mu_{j+1}\}$ that correspond to the structural modes are obtained. These can e.g. be determined using the techniques described in section 6.3.

The mode shapes can then be determined on the basis of the covariance function $\mathbf{\Sigma}(k)$, for $k \geq 0$, of the response of the structure. This covariance function can e.g. be estimated from the p measured records by using an unbiased FFT approach, see Bendat et al. [14] or Brincker et al. [18], and its dimension will as such be $p \times p$. The covariance function can be expressed directly in terms of the modally decomposed system, see e.g. Brincker et al. [17] and Pandit [84]

$$\mathbf{\Sigma}(k) = \sum_{j=1}^{2n} \boldsymbol{\sigma}_j \mu_j^k \tag{6.34}$$

where $\boldsymbol{\sigma}_j$ are $p \times p$ modal weight matrices. The ith row of $\boldsymbol{\sigma}_j$ can be shown to be proportional to the ith mode shape $\mathbf{\Phi}_i$, see Pandit [84]. Therefore, if the weight matrices $\boldsymbol{\sigma}_j$ can be determined from $\mathbf{\Sigma}(k)$ the p scaled mode shapes can be estimated

directly. By setting the $2n$ eigenvalues μ_j in (6.34) equal to the n complex conjugated pairs of structural eigenvalues from the ARMA model, the weight matrices can be determined from (6.34) by the following equation system

$$\begin{bmatrix} \boldsymbol{\Sigma}(0) \\ \boldsymbol{\Sigma}(1) \\ . \\ . \\ \boldsymbol{\Sigma}(m-2) \\ \boldsymbol{\Sigma}(m-1) \end{bmatrix} = \begin{bmatrix} \boldsymbol{I} & \boldsymbol{I} & . & . & \boldsymbol{I} & \boldsymbol{I} \\ \boldsymbol{I}\mu_1 & \boldsymbol{I}\mu_2 & . & . & \boldsymbol{I}\mu_{2n-1} & \boldsymbol{I}\mu_{2n} \\ . & . & . & . & . & . \\ . & . & . & . & . & . \\ \boldsymbol{I}\mu_1^{m-2} & \boldsymbol{I}\mu_2^{m-2} & . & . & \boldsymbol{I}\mu_{2n-1}^{m-2} & \boldsymbol{I}\mu_{2n}^{m-2} \\ \boldsymbol{I}\mu_1^{m-1} & \boldsymbol{I}\mu_2^{m-1} & . & . & \boldsymbol{I}\mu_{2n-1}^{m-1} & \boldsymbol{I}\mu_{2n}^{m-1} \end{bmatrix} \begin{bmatrix} \boldsymbol{\sigma}_1 \\ \boldsymbol{\sigma}_2 \\ . \\ . \\ \boldsymbol{\sigma}_{2n-1} \\ \boldsymbol{\sigma}_{2n} \end{bmatrix} \tag{6.35}$$

which for short can be written as

$$\boldsymbol{S} = \boldsymbol{M}\boldsymbol{W} \tag{6.36}$$

The weights can then be found as $\boldsymbol{W} = \boldsymbol{M}^{-1}\boldsymbol{S}$. The inverse of the matrix $\boldsymbol{M}$ can only be calculated for $m = 2n$. If $m > 2n$ the inverse is replaced by the pseudo-inverse of $\boldsymbol{M}$. The result is $2n$ estimates of the p scaled mode shapes. These $2n$ estimates can then be averaged to increase the numerical accuracy. This way of obtaining the mode shapes on the basis of an ARMA model and estimates of the covariance function from the measured records is in Brincker et al. [17] referred to as a hybrid ARMA approach for modal analysis, and it is concluded that this approach works well if the modes are well separated.

6.6 Summary

The purpose of this chapter has been to describe modal analysis using discrete-time parametric time domain models in the field of civil engineering. It has been described how to modally decompose a general discrete-time parametric model and how to obtain the modal parameters on the basis of this decomposition. In this context, it has been verified that the modal decomposition of a general state space realization is also the modal decomposition of the corresponding ARMAV model. In some applications, it is important to have an idea about the accuracy of the estimated modal parameters. It has therefore been shown how to estimate the standard deviations of the estimated natural eigenfrequencies, damping ratios, and mode shapes. These uncertainty measures rely on the estimated covariance matrix of the model parameters. This covariance matrix is easy to estimate using a PEM identification approach.

One of the difficulties in using parametric models for system identification is that the selection of physical and nonphysical modes in general must be performed by the user. In this context, it has been considered how to distinguish between these two types of modes. It has been shown that one of the most efficient ways to determine

physically related modes is by plotting all estimated models in a stability diagram. Such a diagram can e.g. incorporate a priori knowledge about e.g. the maximum damping of the structural modes. It can also incorporate information about the mode shapes through e.g. the MAC.

As a part of a modal analysis a spectrum analysis is often performed. For stochastically excited systems, spectrum analysis is a powerful way to visualize the dynamic properties of the structural system itself and the excitation. Traditionally, spectrum analysis has been based of the FFT. However, having estimated a parametric model it is also possible to obtain the spectral densities directly from the estimated model parameters and the associated innovation covariance matrix.

Finally, it might be that at some prior state a modal analysis of a structure have been made using an univariate parametric model. One reason could be, that only one sensor has been mounted on the structure in the prior analysis. However, if a more complex analysis is desired at a later state using several sensors, then all modal parameters can be estimated in a fast way by using the prior information about the structural eigenvalues. If this prior information is combined with a covariance estimation approach applied to the new measurements, then the mode shapes of the structural modes can be estimated rapidly. A way to obtain the covariance estimates is by using an unbiased FFT approach. This modal analysis approach is referred to as a hybrid approach, since it involves ARMA model estimation as well as covariance estimation using e.g. FFT.